General Framework for Georeferencing and Interpretation of Multi-Resolution LiDAR Data for Fine-Scale Forest Inventory

Hazem Hanafy[1], Sang-Yeop Shin[1], Aser M. Eissa[1], Youssef Hany[1], Sangyoon Park[1], Songlin Fei[2], and Ayman Habib[1]

[1] Lyles School of Civil and Construction Engineering, Purdue University, West Lafayette, USA - (hhanafy, shin337, eissaa, yaboelma, park1858, ahabib) @purdue.edu
[2] Department of Forestry and Natural Resources, Purdue University, West Lafayette, USA - sfei@purdue.edu

Keywords: Multi-Resolution LiDAR point cloud, Individual tree segmentation, Forest biometrics

Abstract:

Accurate forest inventory is critical for sustainable management, ecological assessment, and biomass estimation. Combining near-proximal and proximal Light Detection and Ranging (LiDAR) data produces point clouds that fully capture the forest structure. This study presents a unified framework for processing multi-resolution LiDAR data to extract key forest attributes, including tree location, height, and diameter at breast height (DBH). The proposed methodology integrates LiDAR data captured by Unmanned Aerial Vehicles (UAVs) and BackPack systems for canopy structure delineation and fine-scale understory mapping, enhancing the accuracy of tree segmentation and biometrics estimation. A multi-stage processing pipeline is developed, incorporating adaptive ground removal, intensity/geometry-based filtering for woody part separation, and layered density-based spatial clustering of applications with noise (DBSCAN) to mitigate over-segmentation. Additionally, an image-LiDAR linking strategy is introduced as a precursor for tree species identification by associating segmented trees with UAV and BackPack imagery. The proposed approach is evaluated in a plantation, demonstrating an F1-score of 100% for tree detection and a 3.1 cm root mean square error (RMSE) for DBH estimation. The results highlight the reliability of the proposed framework for accurately detecting trees and estimating their DBH. Furthermore, by combining geometric information from LiDAR with the rich semantic information in captured imagery, the proposed image-LiDAR linking strategy shows its potential for tree species identification. The effectiveness of multi-source LiDAR integration for forest inventory applications, offers a scalable solution for large-scale forest monitoring. Future work will focus on improving tree segmentation in complex forest environments and leveraging machine learning models for automated species classification.

1. Introduction

Fine-resolution forest inventory is essential for evaluating forest health, biomass distribution, and carbon storage, forming a foundation for sustainable forest management. Accurate inventory data informs policy decisions aimed at tackling climate change, preserving biodiversity, and optimizing forest resources (Lin et al., 2022). Traditionally, forest assessments depended on manual measurements, which are time-consuming and expensive. However, advancements in remote sensing, particularly Light Detection and Ranging (LiDAR) technology, have transformed forest data collection. Research has highlighted the effectiveness of LiDAR in various inventory applications, including detecting individual trees, estimating tree height, analysing canopy structure, and assessing above-ground biomass (Chen et al., 2021; Ganz et al., 2019; Lin et al., 2021; Pirotti et al., 2017; Revenga et al., 2022; Wallace et al., 2014, 2012).

Near-proximal and proximal LiDAR technologies, such as Unmanned Aerial Vehicles (UAVs) and BackPack mobile LiDAR systems, provide high-resolution data for forest inventory. UAV LiDAR, which operates above the canopy, provides canopy structure data while maintaining stable Global Navigation Satellite System (GNSS) signal connectivity, making it particularly useful for mapping tree crowns and overall forest structure. However, the nature of data acquisition from aerial vehicles limits their ability in capturing details beneath dense foliage, such as diameter at breast height (DBH) and stem volume. On the other hand, BackPack LiDAR, used within the forest understory, captures fine-scale details of trunks, ground vegetation, and other structural elements crucial for a thorough forest assessment (Shao et al., 2024). Integrating UAV and BackPack LiDAR data enhances inventory accuracy by combining canopy-level mapping with below-canopy level structural analysis. Additionally, incorporating Red-Green-Blue (RGB) imagery with LiDAR presents several potential benefits for tree species identification, further expanding its applications in forest ecology.

Many researchers have focused on Mobile Laser Scanning (MLS) for evaluating its accuracy and efficiency in forest inventory applications. Chiappini et al. (2022) evaluated the accuracy of handheld MLS compared to traditional manual measurements for estimating dendrometric variables in a black pine plantation. Their study demonstrated that MLS provides precise estimates of tree height and DBH, offering an efficient alternative to labour-intensive field measurements. Their findings indicate that MLS can achieve comparable accuracy to manual measurements while significantly reducing field survey time, making it a viable tool for large-scale forest inventory applications. Balestra et al. (2024) introduced a UAV image/LiDAR data fusion approach for estimating individual tree carbon stock, highlighting its application in urban green planning and sustainable forest management. This method combines UAV imagery with spherical LiDAR data to enhance tree parameter estimation and improve carbon stock assessments. Their findings show that integrating UAV LiDAR and RGB imagery enhances carbon stock estimation and enables high-resolution tree monitoring in urban areas.

Recent advancements in remote sensing technologies have enabled more efficient and detailed 3D modeling of urban trees, leveraging various sensing methods for improved accuracy. Chiappini et al. (2024) compared the accuracy of 3D urban olive tree models generated using different sensing technologies, including LiDAR sensors on smartphones, photogrammetry, and neural radiance fields (NeRF). Their study demonstrated that smartphone LiDAR can effectively capture tree structure, though photogrammetry and NeRF provided more detailed reconstructions. The findings highlighted the potential of smartphone-based

LiDAR for rapid tree modeling but emphasized the need for hybrid approaches to improve accuracy in complex environments. Gollob et al. (2021) assessed the capability of Apple iPad Pro's integrated LiDAR sensor for measuring forest inventory parameters. Their study evaluated the accuracy of tree height, DBH, and stem volume estimates using this consumer-grade technology. The findings suggest that iPad LiDAR can estimate forest inventory biometrics but with lower accuracy than TLS and MLS, making it better for preliminary assessments and rapid field surveys.

Current limitations in forest inventory applications include the lower accuracy of consumer-grade LiDAR sensors compared to traditional MLS and TLS systems, making them less suitable for high-precision measurements. Additionally, while UAV and smartphone-based approaches show promise, they often require hybrid methods or data fusion techniques to improve accuracy in complex environments such as dense forests and urban settings. This study proposes a unified framework for deriving key forest inventory attributes, including tree location, height, and DBH, while also proposing an image-LiDAR linking strategy that can potentially be used for tree species classification. Furthermore, the proposed pipeline can deal with processing both single-source and multi-source LiDAR data across extensive forested areas. By addressing current challenges in multi-platform LiDAR integration and automation, this research aims to improve large-scale forest monitoring, supporting sustainable management and conservation efforts. The remainder of this paper is structured as follows: Section 2 introduces the proximal and near proximal mobile mapping systems, study sites, and acquired datasets used in this study; Sections 3 and 4 demonstrate the overall methodology and the experimental results; Lastly, Section 5 summarizes the findings of the research and recommendations for future work.

2. Data Acquisition Systems and Study Site

The point clouds used in this study were collected by two different platforms: 1) UAV and 2) BackPack LiDAR systems. The UAV system in Figure **1** is equipped with an Ouster OS1-128 LiDAR sensor (Ouster, 2025), a Sony RX1RII camera (Sony, 2024b), and an Applanix APX15 v3 GNSS/INS unit (Applanix, 2025). The GNSS/INS unit records Inertial Measurement Unit (IMU) data at a rate of 200 Hz, ensuring precise positioning and orientation tracking. This system can achieve a positional accuracy around ±5 cm and orientation accuracy of ±0.025° for roll/pitch angles and ±0.080° for heading in open-sky conditions.

The Backpack LiDAR system, shown in Figure **2**, includes a Velodyne VLP-16 LiDAR sensor (Velodyne, 2025) and a Sony α7R II digital camera (Sony, 2024b) for integrated imaging and spatial data collection. BackPack data georeferencing was realized using a Novatel SPAN-CPT GNSS/INS unit (Novatel, 2024), ensuring accurate positioning and orientation. The system records IMU data at a rate of 100 Hz, achieving a post-processing positional accuracy of ±1 to ±2 cm and orientation accuracy of ±0.008° for roll/pitch and ±0.026° for heading.

A black walnut plantation, located near Purdue University in West Lafayette, IN, USA serves as the study site for this work. The site measures approximately 100 m × 75 m, as illustrated in Figure 3. The plantation layout consists of 16 rows and 12 columns, with an average tree spacing of 4.5 m. The average tree height in this area is approximately 25 m.

For the UAV, data collection took place during the leaf-on season in September 2024. The UAV operated at an altitude of 50 m above ground, flying at a speed of 3.6 m/s along seven flight lines in the East-West direction, with a lateral distance of 15 m between adjacent flights. The point cloud was reconstructed using an off-nadir angle of ±70°, achieving a 97% overlap between adjacent flight lines. For the BackPack system, data collection was conducted during the leaf-off season in March 2024. The operator traversed the site along 13 tracks in the East-West direction. The datasets from both platforms were integrated using the F^2-LSLAM algorithm (Zhao, 2023) to enhance spatial consistency and alignment between the datasets, ensuring a seamless representation of the study area. Table 1 summarizes the specifications of the data acquisition systems and the collected data.

System	UAV System	BackPack System
Sensors & Units	Ouster OS1-128 LiDAR, Sony RX1RII Camera, Applanix APX15 v3 GNSS/INS	Velodyne VLP-16 LiDAR, Sony α7R II Camera, Novatel SPAN-CPT GNSS/INS
IMU Data Frequency	200 HZ	100 HZ
Positional Accuracy	±5 cm	±1 to ±2 cm
Orientation Accuracy	±0.025° (roll/pitch), ±0.080° (heading)	±0.008° (roll/pitch), ±0.026° (heading)
Collection Season	Leaf-on (September 2024)	Leaf-off (March 2024)
Flight/Survey Details	Altitude: 50 m, Speed: 3.6 m/s, 7 E-W flight lines, 15 m lateral distance	13 E-W tracks

Table 1. Systems specifications summary

Figure 1. UAV LiDAR system.

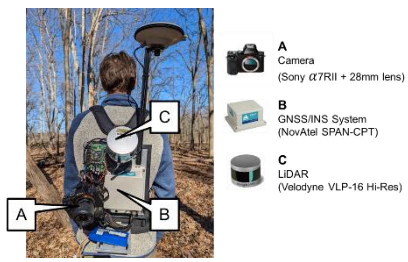

Figure 2. BackPack LiDAR system.

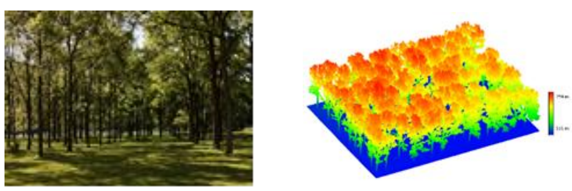

(a) (b)

Figure 3. Black walnut area: (a) a sample image showing the study site and (b) combined UAV/BackPack LiDAR point clouds (colored by height).

3. Methodology

Figure 4 illustrates the workflow of the proposed forest inventory pipeline and LiDAR image linking algorithm, which will be used as a precursor for tree species identification. The workflow starts with a pre-processing step to handle large datasets and remove ground points. Next, height normalization is applied to facilitate tree segmentation and deriving individual tree location, DBH, and height. Various filtering techniques are applied to separate connected tree canopy, improving segmentation accuracy. Finally, clustering and quality control address tree over-segmentation, ensuring reliable forest inventory metrics. The details of the methodology are explained in the following subsections.

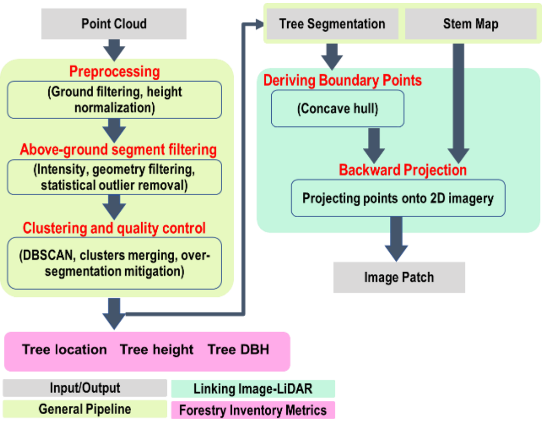

Figure 4. Illustration of the proposed workflow.

3.1 Forest Inventory Pipeline

3.1.1 Pre-processing and Above-Ground Filtering

The workflow begins with ground filtering using an adaptive cloth simulation algorithm (Lin et al., 2021), which conducts ground and non-ground separation while generating a Digital Terrain Model (DTM) as shown in Figure 5. The above-ground point cloud undergoes a series of filtering processes to enhance segmentation accuracy. A two-step filtering process is applied to separate tree woody parts from foliage and mitigate the effects of canopy connectivity. First, intensity filtering removes foliage using an adaptive threshold derived through Otsu’s strategy (Otsu, 1979), effectively isolating high-intensity woody components. Second, geometric filtering partitions the point cloud into prisms of predefined dimensions, allowing for structural analysis based on a linearity metric derived through variance-covariance analysis of individual prisms. Points within prisms exhibiting strong linear characteristics are assumed to represent tree trunks and are retained.

Following these steps, a statistical outlier removal (SOR) is applied to refine the point cloud by eliminating noise while preserving key woody parts. Figure 6 shows a sample tree in the original point cloud and the outcome of each filtering step. One should note that points lower than 5 meters above the ground are not included in the filtering process, which aims at minimizing interlocking between adjacent trees in the upper canopy (i.e., we ensure that the tree trunks are always retained). This approach ensures the retention of essential data for precise tree identification.

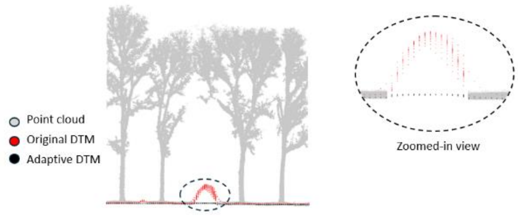

Figure 5. Illustration of generated DTMs derived from the original (red) and adaptive (black) cloth simulation filters, with a zoomed-in section showing an artificial peak in the DTM from the original cloth simulation filter.

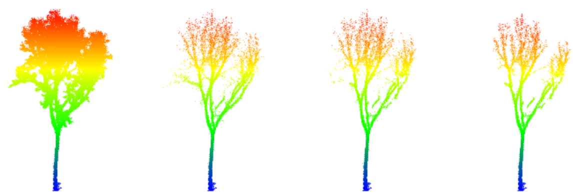

(a) (b) (c) (d)

Figure 6. Filtering process for a sample tree showing: (a) original point cloud, (b) woody points after intensity filtering, (c) result after geometry filtering, and (d) remaining point cloud after outlier removal.

3.1.2 Clustering and Individual Tree Localization

Tree segmentation is performed using the traditional DBSCAN algorithm (Ester, 1996) in a layered approach rather than applying it to the entire point cloud at once. This double-layer strategy ensures that even when adjacent tree canopies remain connected, as shown in Figure 7(a), the trunk layer remains isolated. This separation allows for accurate identification of individual tree clusters. To refine the segmentation, adjacent clusters across multiple layers are merged based on centroid proximity and eigenvector alignment as shown in Figure 7(b). Tree locations are determined by analysing the sum of elevation values within a 2D grid representation of the segmented points, specifically for the lower section with a given threshold above ground for each segment. The presence of trees is identified by having local maxima in the elevation sum, with peaks corresponding to individual tree location. To eliminate false positives, a trunk continuity check is performed. This involves slicing each trunk into multiple intervals, evaluating the point distribution within each slice and calculating the percentage of completeness along the trunk’s height. This process ensures that only well-defined tree trunks are retained. To mitigate over-segmentation, falsely segmented clusters are removed by verifying the presence of a corresponding tree location. Clusters without a matching tree location are considered over-segmented and subsequently excluded as shown in Figure 7(c). After the final segmentation of woody parts, individual tree locations are further refined by defining the tree axis and identifying its intersection with the DTM to determine the final tree position.

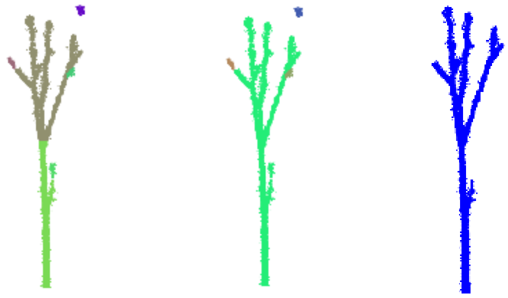

(a) (b) (c)

Figure 7. Illustration of layered DBSCAN and over-segmentation mitigation showing: (a) clustering result for the multiple layers, (b) merged clusters based on proximity, and (c) final segmented woody part after over-segmentation mitigation.

3.1.3 Final Tree Segmentation and Biometrics Extraction

Key tree metrics including location, DBH, and height are derived from the segmented clusters. DBH is estimated through circle fitting for a cross-section between 1.4 m and 1.5 m from the ground, while ensuring sufficient point density for accurate estimation. Filtered points, previously removed during intensity and geometry filtering (Section 3.1.1), are iteratively reintegrated in small increments, restoring only points near the segmented woody structure. This iterative region-growing process retains essential canopy points while minimizing the inclusion of distant noise. The reintegration occurs based on a 10 cm proximity criterion per iteration, enabling controlled adjustments that maintain segmentation accuracy to represent entire tree structure. Figure 8 illustrates an example of the reintegration process, where the initially segmented woody structure shown in Figure 8(a), and the reintegrated points every 10 iterations represented in different colors as shown in Figure 8(b-d). Finally, tree height is determined from the highest and lowest points within each cluster using the normalized height point cloud. This process enhances tree isolation while preserving critical structural details necessary for accurate forest inventory analysis. Final segmented tree together with derived metrics are shown in Figure 9.

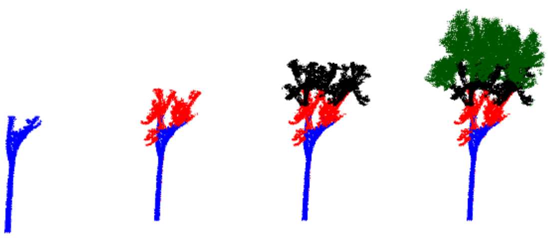

(a) (b) (c) (d)

Figure 8. Iterative reintegration of filtered points into the segmented woody structure: (a) segmented woody structure after over-segmentation mitigation, (b) reintegrated points in red after 10 iterations, (c) reintegrated points in black after 20 iterations, and (d) final reconstructed tree with the reintegrated points beyond 20 iterations in green.

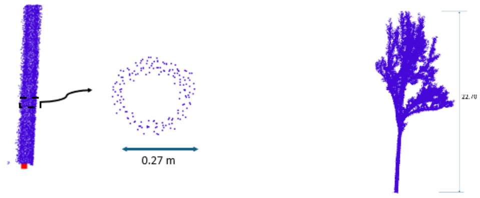

(a) (b)

Figure 9. Derived tree biometrics: (a) tree location represented by the red square together with the cross section used for DBH estimation and (b) segmented tree with the estimated height.

3.1.4 UAV/BackPack Image-LiDAR Linking Strategy

In this study, an image-LiDAR linking strategy is proposed to generate image patches for each tree from both the UAV and BackPack systems. For UAV image patch generation, points above the 90th percentile height for each segmented tree are isolated, as presented in Figure 10(a). A concave hull (Park et al., 2021) is then applied to define their boundary, as illustrated in Figure 10(b). Figure 10(c) shows the back-projection of the derived boundary marked in red onto 2D imagery. Figure 10(d) presents the final UAV image patch, preserving only the image region within the concave hull. For the BackPack system, a similar procedure is applied, but only tree trunk points are considered, as shown in Figure 11(a). Finally, an image patch from the BackPack system is generated, with a buffer applied to its edges to ensure that bark features remain fully visible, as depicted in Figure 11(b).

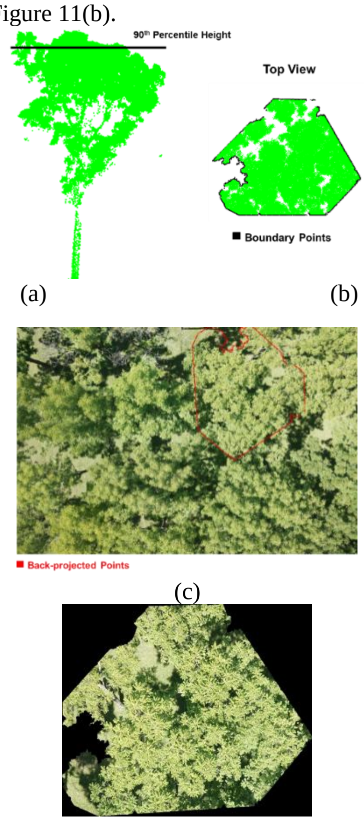

(a) (b) (c) (d)

Figure 10. Illustration of (a) individually-segmented tree points showing the 90th percentile height, (b) isolated points that are above 90th percentile height with their boundary, (c) boundary points back-projected onto 2D imagery, and (d) generated image patch.

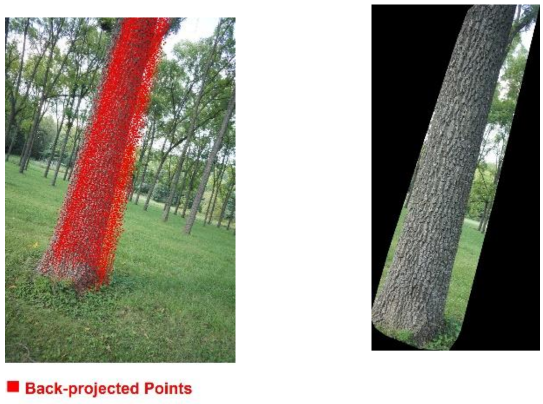

(a) (b)

Figure 11. Illustration of (a) tree trunk points back-projected onto 2D imagery and (b) generated image patch.

4. Experimental Results

This section presents the experimental evaluation of the proposed method. The primary objective of the experiments is to assess the pipeline’s effectiveness in tree detection by establishing True Positives (TP), False Positives (FP), False Negatives (FN) when comparing the results with reference data. Also, the RMSE, characterizing the differences between the estimated DBH values from the proposed strategy and reference data measured in the field using vernier callipers, is reported. To evaluate the pipeline’s performance, the proposed method was tested in a plantation area, where the uniform tree spacing and minimal undergrowth provide a controlled environment for validation. This setting allows for a clear assessment of detection accuracy and diameter measurements, ensuring that the evaluation focuses on the method’s effectiveness without additional variability introduced by complex forest structures. Starting with the pre-processing step, the point cloud is separated into ground and above ground while generating a DTM, which will be used to normalize the point cloud elevation for accurate tree segmentation and detection as shown in Figure 12.

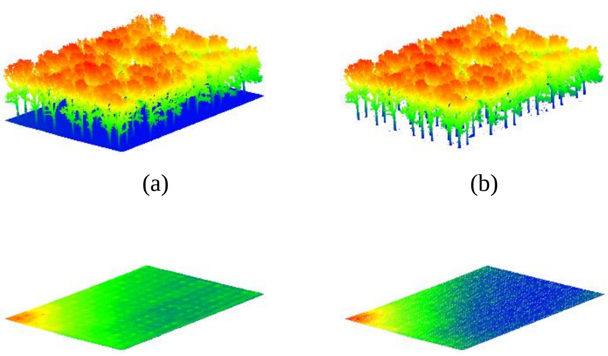

(a) (b) (c) (d)

Figure 12. Ground non-ground separation: (a) original point cloud, (b) above ground point cloud, (c) bare earth point cloud, and (d) digital terrain model.

The next step involves filtering the point cloud to reduce canopy interlocking. As shown in Figure 13, intensity-based filtering, geometry-based retention of woody parts, and SOR noise removal effectively reduce crown overlap by eliminating noise and canopy connections between adjacent trees. This refinement enhances individual tree isolation, leading to more accurate segmentation and better downstream analysis.

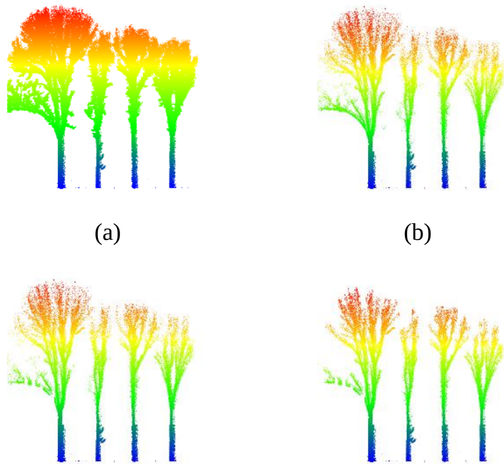

(a) (b) (c) (d)

Figure 13. Filtering and outlier removal steps: (a) original point cloud, (b) intensity filtering results, (c) geometry filtering results, and (d) remaining point cloud after statistical outlier removal.

The clustering and merging approach enhanced tree segmentation accuracy by reducing over-segmentation, particularly in canopy regions. As illustrated in Figure 14(a), the initial layered clustering results show multiple fragmented clusters representing different tree segments. However, as shown in Figure 14(b), most of these initially fragmented clusters were successfully integrated, minimizing redundant detections of individual trees. Without this merging step, multiple detections for a single tree would have occurred, leading to over-segmentation. After the merging process, tree detection was conducted on each cluster. Over-segmented clusters lacking a detected trunk location were reassigned to the nearest valid tree, ensuring a more accurate and cohesive segmentation. This refinement produced a complete tree structure, as depicted in Figure 15(a). Consequently, 92 trees were identified within the study area, as shown in Figure 15(b). The mitigation of over-segmentation enhanced segmentation consistency and reduced false positives, improving the overall accuracy of tree delineation. Additionally, the incremental reintegration of filtered points further enhanced the representation of tree structures. The most significant improvements were observed in dense and overlapping tree regions, where the proposed method achieved more accurate delineation of individual trees. Unlike conventional segmentation techniques, which often result in false boundary lines between closely spaced trees—resulting in unnecessary fragmentation, the proposed approach preserves structural continuity ensuring a more natural and cohesive segmentation, as shown in Figure 16. The extracted forest inventory metrics including tree height and DBH are presented in Figure 17, where each individual tree is visualized with its corresponding height and DBH value.

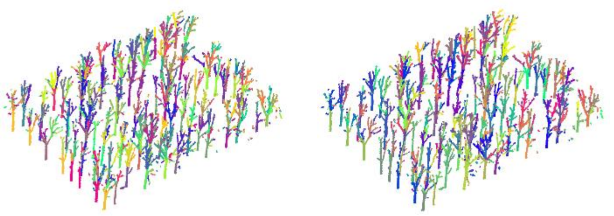

(a) (b)

Figure 14. Illustration of (a) layered DBSCAN clustering and (b) clusters after merging based on proximity.

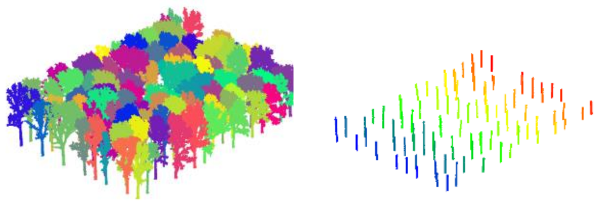

(a) (b)

Figure 15. Illustration of (a) individual tree segmentation results (randomly colored by tree ID) and (b) stem mapping (colored by tree ID).

(a) (b)

Figure 16. Illustration of sample segmented trees: (a) perspective view of segmented trees and (b) top view.

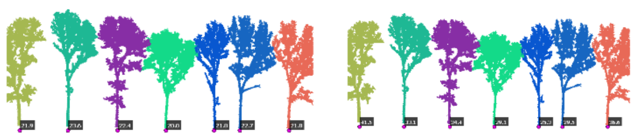

(a) (b)

Figure 17. Derived forest inventory metrics for individual trees: (a) individually segmented trees with estimated tree height in m, and (b) individually segmented trees with estimated DBH in cm.

The detected trees were compared with reference data to evaluate the quality of tree detection by determining TP, FP, and FN. Additionally, the RMSE characterizing the differences between the estimated and reference DBH measurements in the field was calculated. The results of this evaluation are summarized in Tables 2 and 3. The experimental results for tree detection achieved an F1-Score of 100% indicating that the approach had flawless precision and recall for the test area. The estimated tree DBH values exhibited an RMSE of 3.1 cm. While this indicates that the approach performs well, the median difference of 3.1 cm suggests a systematic bias relative to the reference data. This bias is primarily attributed to partial occlusion of tree trunks. Compared to manual calliper measurements, the proposed method tends to slightly underestimate DBH, likely due to inconsistencies in scan coverage. Figure 18 presents an example of the generated image patches derived from both UAV and BackPack systems. The quality of the generated image patch relies on the georeferencing quality of both the image and LiDAR data.

Total number of trees	TP	FP	FN	Precision (%)	Recall (%)	F1-score (%)
92	92	0	0	100	100	100

Table 2. Tree detection evaluation results

Total number of trees	Min (cm)	Max (cm)	Median (cm)	STD (cm)	RMS (cm)
92	0.1	-4.3	-3.1	0.7	3.1

Table 3. DBH quality analysis using reference data

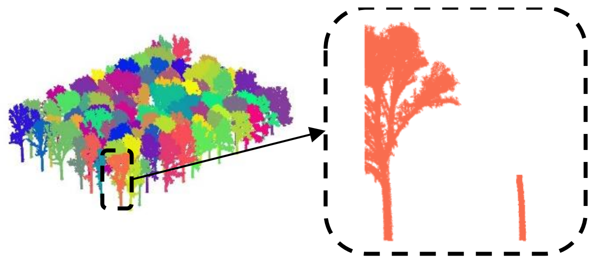

(a)

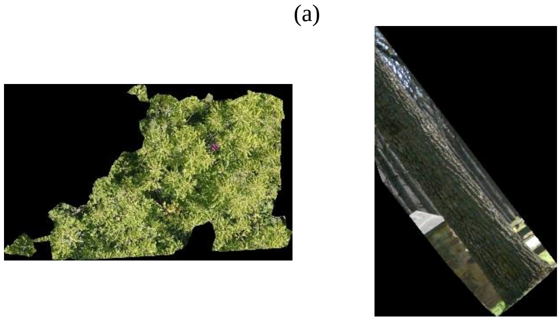

(b) (c)

Figure 18. An example illustrating (a) an individually segmented tree and stem map displaying the generated image patches from (b) UAV showing the highest point highlighted by a magenta cross and (c) BackPack showing canopy and tree trunk features, respectively.

5. Conclusions and Recommendations for Future Work

This study presents a unified framework for deriving key forest inventory attributes by integrating multi-resolution LiDAR data from UAV and BackPack systems. The proposed methodology enhances individual tree segmentation through adaptive filtering, layered clustering, and an iterative reintegration strategy to retrieve filtered points and preserve entire tree structure. Experimental evaluation in a plantation environment demonstrated an F1-score of 100% for tree detection and a 3.1 cm RMSE for DBH estimation, validating the accuracy and reliability of the approach. Additionally, the introduced image-LiDAR linking strategy will facilitate tree species identification by combining structural information from LiDAR with semantic cues from imagery. While the evaluation was conducted in a plantation setting with uniform spacing and minimal undergrowth, the methodology is designed to be adaptable to more complex forest environments and different seasonal conditions. By leveraging its robust segmentation and feature extraction capabilities, the approach holds promise for large-scale forest inventory across diverse ecological settings, supporting sustainable forest management and monitoring.

While the proposed pipeline demonstrates high accuracy in a plantation setting, further validation on diverse datasets is necessary to assess its generalizability across different forest environments and seasonal conditions. Future work will focus on testing the approach in natural forests with varying tree densities and structures to evaluate its robustness and adaptability and exploring learning-based approaches for automated tree species classification using the generated image patches and segmented tree points.

Acknowledgment

This work is partially supported by the USDA NRCS (award #NR233A750004G044) and USDA NIFA (award #2023-68012-38992 and #2024-67021-42879). The views and conclusions contained herein are those of the authors and should not be interpreted as representing the official policies, either expressed or implied, of the U.S. Government, NRCS, or NIFA. The U.S. Government is authorized to reproduce and distribute reprints for governmental purposes notwithstanding any copyright annotation therein.

References

Applanix, 2024., URL https://www.applanix.com/downloads/products/specs/APX15_UAV.pdf (29 January 2025)

Balestra, M., Choudhury, M. A. M., Pierdicca, R., Chiappini, S., & Marcheggiani, E., 2024. UAV-Spherical Data Fusion Approach to Estimate Individual Tree Carbon Stock for Urban Green Planning and Management. *Remote Sensing*, 16(12), 2110.

Chen, X., K. Jiang, Y. Zhu, X. Wang, T. Yun., 2021. Individual tree crown segmentation directly from UAV-borne LiDAR data using the PointNet of deep learning. *Forests*, 12, 131.

Chiappini, S., Balestra, M., Giulioni, F., Marcheggiani, E., Malinverni, E. S., & Pierdicca, R., 2024. Comparing the accuracy of 3D urban olive tree models detected by smartphone using LiDAR sensor, photogrammetry and NeRF: a case study of’Ascolana Tenera’in Italy. *ISPRS Annals of the Photogrammetry, Remote Sensing and Spatial Information Sciences*, 10, 61-68.

Chiappini, S., Pierdicca, R., Malandra, F., Tonelli, E., Malinverni, E. S., Urbinati, C., & Vitali, A., 2022. Comparing Mobile Laser Scanner and manual measurements for dendrometric variables estimation in a black pine (Pinus nigra Arn.) plantation. *Computers and Electronics in Agriculture*, 198, 107069.

Ester, M., Kriegel, H.-P., Sander, J., Xu, X., & others., 1996. A density-based algorithm for discovering clusters in large spatial databases with noise. In *kdd* (Vol. 96, pp. 226–231)

Ganz, S., Y. Käber, P. Adler., 2019. Measuring tree height with remote sensing—A comparison of photogrammetric and LiDAR data with different field measurements. *Forests*, 10, 694.

Gollob, C., Ritter, T., Kraßnitzer, R., Tockner, A., & Nothdurft, A., 2021. Measurement of forest inventory parameters with Apple iPad pro and integrated LiDAR technology. *Remote Sensing*, 13(16), 3129.

Lin, Y.C., Liu, J., Fei, S., Habib, A., 2021. Leaf-off and leaf-on uav lidar surveys for single-tree inventory in forest plantations. *Drones*.

Lin, Y. C., Shao, J., Shin, S. Y., Saka, Z., Joseph, M., Manish, R., ... & Habib, A., 2022. Comparative analysis of multi-platform, multi-resolution, multi-temporal LiDAR data for forest inventory. *Remote Sensing*, 14(3), 649.

Novatel. 2025., URL: https://novatel.com/support/previous-generation-products-drop-down/previous-generation-products/span-cpt. (29 January 2025)

Otsu, N. 1979., A threshold selection method from gray-level histograms. *IEEE Transactions on Systems, Man, and Cybernetics*, 9, 62–66.

Ouster., 2025., URL: https://ouster.com/insights/blog/introducing-the-os-1-128-lidar-sensor. (29 January 2025)

Pan, Y., Birdsey, R. A., Fang, J., et al., 2011. A large and persistent carbon sink in the world’s forests. *Science*, 333(6045), 988-993.

Park, J. S., & Oh, S. J., 2012. A new concave hull algorithm and concaveness measure for n-dimensional datasets. *Journal of Information science and engineering*, 28(3), 587-600.

Pirotti, F., Kobal, M., Roussel, J.R., 2017. A Comparison of Tree Segmentation Methods Using Very High Density Airborne Laser Scanner Data. *The International Archives of the Photogrammetry, Remote Sensing and Spatial Information Sciences* XLII-2/W7, 285–290.

Revenga, J. C., K. Trepekli, S. Oehmcke, R. Jensen, L. Li, C. Igel, F. C. Gieseke, T. Friborg., 2022. Above-ground biomass prediction for croplands at a sub-meter resolution using UAV–LiDAR and machine learning methods. *Remote Sensing*, 14, 3912.

Rusu, R. B., N. Blodow, Z. C. Marton, M. Beetz., 2008. Aligning point cloud views using persistent feature histograms. 2008 IEEE/RSJ International Conference on Intelligent Robots and Systems (IROS), IEEE, pp. 3384–3391.

Shao, J., Lin, Y.-C., Wingren, C., Shin, S.-Y., Fei, W., Carpenter, J., Habib, A., Fei, S., 2024. Large-scale inventory in natural forests with mobile LiDAR point clouds. *Science of Remote Sensing* 100168.

Sony, 2024a., URL https://www.sony.com/za/electronics/cyber-shot-compact-cameras/dsc-rx1rm2 (13 November 2024).

Sony, 2024b., URL https://electronics.sony.com/imaging/interchangeable-lens-cameras/full-frame/p/ilce7rm2-b?srsltid=AfmBOoq-_HX6DDkc2WBYhtk74afnIdJiZ1lFc26PnopJNGneIq0xUCA4. (13 November 2024)

Velodyne, 2025. URL https://ouster.com/products/hardware/vlp-16 (29 January 2025)

Wallace, L., A. Lucieer, C. Watson, D. Turner., 2012. Development of a UAV-LiDAR system with application to forest inventory. Remote Sensing, 4, 1519–1543.

Wallace, L., A. Lucieer, C. S. Watson., 2014. Evaluating tree detection and segmentation routines on very high-resolution UAV LiDAR data. IEEE Transactions on Geoscience and Remote Sensing, 52, 7619–7628.

Zhao, C., T. Zhou, S. Fei, A. Habib., 2023. Forest feature LiDAR SLAM (F2-LSLAM) and integrated scan simultaneous trajectory enhancement and mapping (IS2-TEAM) for accurate forest inventory using backpack systems. The International Archives of the Photogrammetry, Remote Sensing and Spatial Information Sciences, 48, 1823–1830.

Zhou, T., Ravi, R., Lin, Y. C., Manish, R., Fei, S., & Habib, A., 2023. In Situ Calibration and Trajectory Enhancement of UAV and Backpack LiDAR Systems for Fine-Resolution Forest Inventory. Remote Sensing, 15(11), 2799.